Smooth muscle fascicular reorientation is required for esophageal morphogenesis and dependent on Cdo

Anthony I. Romer,[1,2] Jagmohan Singh,[3] Satish Rattan,[3] and Robert S. Krauss[1,2]

[1]Department of Developmental and Regenerative Biology, and [2] Graduate School of Biomedical Sciences, Mount Sinai School of Medicine, New York, NY 10029
[3]Department of Medicine, Division of Gastroenterology and Hepatology, Jefferson Medical College, Thomas Jefferson University, Philadelphia, PA 19107

Postnatal maturation of esophageal musculature involves proximal-to-distal replacement of smooth muscle with skeletal muscle by elusive mechanisms. We report that this process is impaired in mice lacking the cell surface receptor Cdo and identify the underlying developmental mechanism. A myogenic transition zone containing proliferative skeletal muscle precursor cells migrated in a proximal–distal direction, leaving differentiated myofibers in its wake. Distal to the transition zone, smooth muscle fascicles underwent a morphogenetic process whereby they changed their orientation relative to each other and to the lumen. Consequently, a path was cleared for the transition zone, and smooth muscle ultimately occupied only the distal-most esophagus; there was no loss of smooth muscle. *Cdo*$^{-/-}$ mice were specifically defective in fascicular reorientation, resulting in an aberrantly proximal skeletal–smooth muscle boundary. Furthermore, *Cdo*$^{-/-}$ mice displayed megaesophagus and achalasia, and their lower esophageal sphincter was resistant to nitric oxide–induced relaxation, suggesting a developmental linkage between patterning and sphincter function. Collectively, these results illuminate mechanisms of esophageal morphogenesis and motility disorders.

Introduction

The esophagus transports food from the pharynx to the stomach by waves of proximal-to-distal peristaltic contractions. Ingesta empty from the esophagus into the stomach by the transient relaxation of tonic smooth muscle in the lower esophageal sphincter (LES). Swallowing initiates a circuit that activates neurons in the swallowing center of the brain stem, which send projections via the vagus nerve to synapse with neurons in the myenteric plexus of the LES (Goyal and Chaudhury, 2008). Smooth muscles of the LES transiently relax in response to nitric oxide (NO) produced by inhibitory myenteric neurons, allowing food to pass into the stomach (Goyal and Chaudhury, 2008).

Achalasia is an esophageal motility disorder characterized by impaired relaxation of the LES and perturbed peristalsis (Park and Vaezi, 2005). In severe cases of achalasia, chronic accumulation of ingesta expands the esophagus, resulting in megaesophagus. The primary defect in achalasia is defective signaling between the nitrergic (NO-producing) inhibitory neurons present in the myenteric plexus and neighboring smooth muscle cells (SMCs) of the LES (Park and Vaezi, 2005; Goyal and Chaudhury, 2010). Although several mutant mouse lines display achalasia, the genetic and/or environmental factors that underlie human achalasia are largely unknown (Goyal and Chaudhury, 2010).

The esophagus is ensheathed by the muscularis externa (ME). In the adult mouse, the ME is composed of skeletal muscle with the exception of a short, broad segment at the esophago–gastric junction (EGJ), including the LES, which is composed of smooth muscle (Samarasinghe, 1972). During mouse embryogenesis, the ME initially comprises only smooth muscle. Skeletal muscle precursors are first detected in the proximal ME at embryonic day (E) 13, and over the next three weeks of life, particularly between postnatal day (P) 0 and P14, smooth muscle is replaced by skeletal muscle in a proximal-to-distal manner such that the adult pattern is nearly completely achieved (Patapoutian et al., 1995; Kablar et al., 2000; Rishniw et al., 2007). A similar process occurs during human esophageal

Correspondence to Robert S. Krauss: Robert.Krauss@mssm.edu

Abbreviations used in this paper: α-SMA, α-smooth muscle actin; β-gal, β-galactosidase; EFS, electrical field stimulation; EGJ, esophago–gastric junction; Hh, Hedgehog; IFA, immunofluorescence analysis; LES, lower esophageal sphincter; ME, muscularis externa; NO, nitric oxide; SA, sarcomeric actin; SMC, smooth muscle cell; SNP, sodium nitroprusside; TZ, transition zone.

The Rockefeller University Press $30.00
J. Cell Biol. Vol. 201 No. 2 309–323
www.jcb.org/cgi/doi/10.1083/jcb.201301005

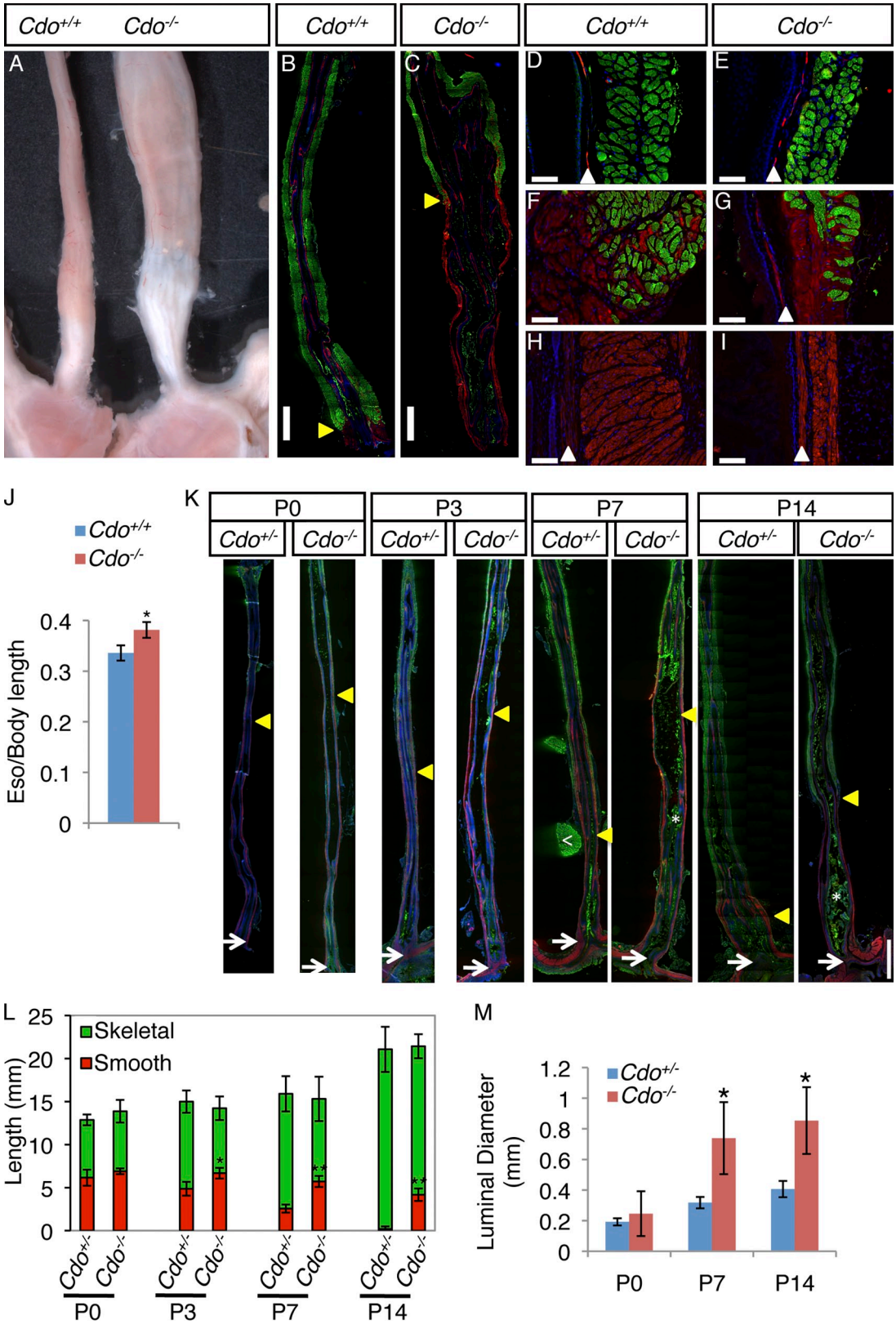

Figure 1. ***Cdo*$^{-/-}$ mice have megaesophagus and display defective proximal-to-distal progression of ME development.** (A) Adult *Cdo*$^{+/+}$ and *Cdo*$^{-/-}$ esophagi. (B–I) Longitudinal sections of adult *Cdo*$^{+/+}$ and *Cdo*$^{-/-}$ esophagi stained with antibodies to α-smooth muscle actin (α-SMA; red) and sarcomeric actin (SA; green) for smooth and skeletal muscles, respectively. (B and C) *Cdo*$^{-/-}$ esophagi have an aberrantly proximally located skeletal–smooth muscle boundary (arrowheads). Only the distal halves of each esophagus are shown (proximal halves have only skeletal muscle). (D and E) The proximal ME of the *Cdo*$^{-/-}$ esophagus is thinner than the control, but has normal appearing skeletal muscle. The α-SMA^{+} layer is the muscularis mucosa (arrowheads). (F and G) SMCs are dispersed with skeletal myofibers around the skeletal–smooth muscle boundary of both *Cdo*$^{+/+}$ and *Cdo*$^{-/-}$ esophagi. (H and I) The distal *Cdo*$^{-/-}$ esophagus has a long, thin extension of smooth muscle instead of the short, broad segment of smooth muscle found in controls. (J) *Cdo*$^{-/-}$

development but the final skeletal–smooth muscle boundary is at the mid-thoracic level, more proximal than in mice (Katori et al., 2010).

Studies on how skeletal muscle replaces smooth muscle have been controversial. It was initially proposed that this occurred via a developmentally programmed transdifferentiation of SMCs into skeletal muscle cells (Patapoutian et al., 1995). However, lineage tracing and other studies argue that transdifferentiation does not occur during maturation of the ME (Zhao and Dhoot, 2000a; Rishniw et al., 2003, 2007). Others have suggested on the basis of ultrastructural analysis that SMCs are removed by apoptosis (Wörl and Neuhuber, 2005), but molecular markers of apoptosis have not been observed (Patapoutian et al., 1995; Kablar et al., 2000; Rishniw et al., 2007). Finally, it has been proposed that smooth muscle replacement occurs by a combination of distal compaction and proximal dispersal of SMCs (Rishniw et al., 2007); mechanisms for such processes are unknown.

Skeletal muscles of the trunk and limbs develop from progenitor cells in the dorsal somite that express the transcription factors Pax3 and Pax7 (Parker et al., 2003; Lagha et al., 2008). $Pax3^+/Pax7^+$ progenitors proliferate, migrate, and commit to the skeletal muscle lineage upon expression of the myogenic bHLH determination factors, Myf5 and MyoD. Committed skeletal myoblasts subsequently express a related bHLH factor, myogenin, which is required for differentiation into syncytial skeletal myofibers that express the skeletal muscle–specific transcriptional program (Parker et al., 2003; Lagha et al., 2008).

Cdo (also called Cdon) is a multifunctional cell surface receptor (Kang et al., 1997). *Cdo* is expressed in the myogenic compartment of the dorsal somite and in developing skeletal muscle masses throughout development (Kang et al., 1998; Mulieri et al., 2000). *Cdo*-null mice display delayed skeletal myogenesis, and primary myoblasts from such animals differentiate defectively in vitro (Cole et al., 2004; Takaesu et al., 2006). Cdo functions to promote skeletal myoblast differentiation as a component of multiprotein cell surface complexes; in particular, it serves as a signaling coreceptor for N-cadherin in the cell–cell adhesion-initiated activation of the promyogenic MAP kinase, p38α (Krauss, 2010; Lu and Krauss, 2010). Cdo also serves as a ligand-binding coreceptor in the Hedgehog (Hh) pathway, promoting signaling via Gli transcription factors (Tenzen et al., 2006; Zhang et al., 2006). $Cdo^{-/-}$ mice display defects in Sonic Hh signaling during embryogenesis with strain-dependent penetrance and severity (Zhang et al., 2006).

We report here that in $Cdo^{-/-}$ mice the replacement of esophageal smooth muscle with skeletal muscle is impaired. Analysis of postnatal esophageal development revealed that between P0 and P14, smooth muscles in the ME undergo a process of fascicular reorientation that drives formation of the mature ME pattern; $Cdo^{-/-}$ mice are specifically defective in this process. We also describe the proximal-to-distal migration of an ME transition zone (TZ) containing skeletal muscle precursor cells. As distal smooth muscle fascicles alter their shape and orientation the TZ follows, leaving skeletal muscle in its wake. There is no intrinsic defect in esophageal skeletal myogenesis in $Cdo^{-/-}$ mice, but due to the impaired reorientation of smooth muscle fascicles, it occurs at an inappropriately proximal location. Finally, $Cdo^{-/-}$ mice have achalasia with megaesophagus. Functional analyses show that SMCs of the $Cdo^{-/-}$ LES fail to relax in response to neuronally or chemically derived NO. Collectively, these results demonstrate that Cdo is required for postnatal patterning of the esophageal musculature and proper esophageal motility, and illuminate mechanisms of esophageal ME morphogenesis and motility disorders.

Results

$Cdo^{-/-}$ mice develop megaesophagus with mispatterned musculature

$Cdo^{-/-}$ mice displayed megaesophagus with 100% penetrance. $Cdo^{-/-}$ esophagi had an enlarged diameter relative to $Cdo^{+/+}$ controls, a dilated lumen engorged with partially digested food, and upon dissection, showed strong, arrhythmic contractions (Fig. 1 A; Videos 1 and 2). Immunofluorescence analysis (IFA) of longitudinal sections of adult esophagi with markers of smooth muscle (α-smooth muscle actin; α-SMA) and skeletal muscle (sarcomeric actin; SA) revealed that $Cdo^{-/-}$ mice have a mispatterned ME, with the skeletal–smooth muscle boundary occurring at an abnormally proximal position (Fig. 1, B and C). Most smooth muscle in the esophagi of wild-type mice was found in a short, broad segment at the EGJ, with a few SMCs dispersed within the skeletal muscle at the skeletal–smooth muscle boundary (Fig. 1, B, F, and H). Distal to the aberrantly proximal boundary in $Cdo^{-/-}$ esophagi there was a long, thin, ectopic extension of smooth muscle that connected to the LES (Fig. 1, C and I). The ME of the proximal $Cdo^{-/-}$ esophagus had skeletal myofibers of normal appearance, but was slightly thinner than controls, presumably due to the megaesophagus phenotype and luminal expansion from chronic accumulation of ingesta (Fig. 1, D and E). Despite its aberrant location, the skeletal–smooth muscle boundary in $Cdo^{-/-}$ esophagi was similar in appearance to that of controls, showing a relatively abrupt change with some SMCs interspersed with skeletal myofibers (Fig. 1 G). When normalized to body length, $Cdo^{-/-}$ esophagi were longer than those of control mice, likely due to the aberrantly

esophagi are longer than $Cdo^{+/+}$ esophagi, as normalized to body length (tip of nose to base of tail); values are means ± SD, $n = 5$. *, $P < 0.005$. (K) Longitudinal sections of P0, P3, P7, and P14 $Cdo^{+/-}$ and $Cdo^{-/-}$ esophagi were stained with antibodies to α-SMA and SA. The location of the distal-most SA^+ cell in each section is denoted by an arrowhead, the LES by an arrow. The white arrowhead in the P7 $Cdo^{+/-}$ section indicates a piece of the SA^+ diaphragm still attached to the esophagus; asterisks in the P7 and P14 $Cdo^{-/-}$ sections indicate ingesta (green), which binds antibody nonspecifically. (L) The distance between the distal-most SA^+ cell and the LES was measured and is represented by the red portion of the histogram bars. Note that the distance decreases progressively with age in $Cdo^{+/-}$ esophagi, but this fails to occur in $Cdo^{-/-}$ esophagi. Values are means ± SD, $n = 3$–4. *, $P < 0.01$; **, $P < 0.001$; with differences referring to the $Cdo^{+/-}$ and $Cdo^{-/-}$ esophagi at a given age. (M) The luminal diameter of $Cdo^{-/-}$ esophagi is larger than that of $Cdo^{+/-}$ esophagi at P7 and P14, but not at P0. Values are means ± SD, $n = 3$. *, $P < 0.04$. Bars: (B, C, and K) 1 mm; (D–I) 0.1 mm.

long distal region of smooth muscle (Fig. 1 J). The morphology of the rest of the gastrointestinal tract was grossly normal. *Cdo*$^{+/-}$ esophagi resembled the wild type and were used as controls.

During the first two weeks after birth, mouse esophageal skeletal muscle replaces smooth muscle in a proximal-to-distal manner, and the final position of the skeletal–smooth muscle boundary is established. To determine when the defects in *Cdo*$^{-/-}$ mice arise, expression of α-SMA and SA was assessed in longitudinal sections taken at P0–P14. The distal-most SA$^+$ cells in these sections were embedded in smooth muscle. Progression of ME development was monitored by measuring the distance from the distal-most SA$^+$ cell to the LES. At P0, this distance was about half the length of the esophagus in both *Cdo*$^{+/-}$ and *Cdo*$^{-/-}$ mice. The overall morphologies of the esophagi were also similar, each showing a long, thin segment of smooth muscle connecting the skeletal–smooth muscle boundary to the LES (Fig. 1, K and L). Measurements at P3, P7, and P14 demonstrated that in control mice, the distance from the distal-most SA$^+$ cell to the LES diminished such that by P14, smooth muscle was found only just proximal to the LES. In contrast, by P3, the distal-most SA$^+$ cell in *Cdo*$^{-/-}$ mice was at a significantly more proximal location than in control animals; this situation was exacerbated over time such that at P14, smooth muscle still occupied the distal ∼20% of *Cdo*$^{-/-}$ esophagi (Fig. 1, K and L). This is very similar to the ME pattern in adult mutant mice and indicates that the defect was both manifested and completed between P0 and P14. Defects in esophageal motility in *Cdo*$^{-/-}$ mice became apparent with the same time course. Accumulated ingesta were seen in mutant esophagi at P3, and the luminal diameter was enlarged by P7 (Fig. 1, K and M).

Cdo is expressed by esophageal skeletal muscle precursors proximally and SMCs distally

During embryonic development, *Cdo* is expressed in skeletal muscle precursors and differentiating skeletal muscle, but not in mature skeletal myofibers. It is also expressed during embryogenesis in the smooth muscle layer of the developing digestive tract (Kang et al., 1998; Mulieri et al., 2000). We examined *Cdo* expression during postnatal development of the ME with a *lacZ* reporter gene knocked into the *Cdo* locus (Cole and Krauss, 2003). At P7, β-galactosidase (β-gal) activity in *Cdo*$^{+/-}$ esophagi was observed in the distal, smooth muscle–containing region of the ME and in the skeletal-to-smooth muscle TZ (Fig. S1, A–C). Differentiated skeletal myofibers in the proximal esophagus did not express *Cdo*. IFA of sections stained with antibodies to β-gal and α-SMA revealed coexpression in the distal region of the ME (Fig. S1 E). β-Gal$^+$ cells were also found in the TZ, and many of these cells coexpressed myogenin, a marker of skeletal myoblast differentiation (Fig. S1 D). The esophageal epithelium was uniformly negative for reporter expression, but rare β-gal$^+$ cells were found within the muscularis mucosa and submucosa (Fig. S1, B and C). Very similar results were obtained by in situ hybridization with a *Cdo* antisense probe (Fig. S1, F and G). Therefore, at the time of ME patterning, *Cdo* was expressed both in skeletal muscle precursor cells and differentiated SMCs.

Cdo expression was similar in the adult esophagus, detected in smooth muscle located distally and by ∼60% of Pax7$^+$ satellite cells (skeletal muscle stem cells) found adjacent to skeletal myofibers (Fig. S1, H–J and L–Q). *Cdo* was also expressed at variable levels by smooth muscle throughout the GI tract with highest levels in the anterior fundus of the stomach (Fig. S1 K). *Cdo* was not expressed in nNOS$^+$ myenteric neurons that innervate tonic smooth muscle in the LES (Fig. S1, R–T). Time-course analyses of reporter activity in whole-mount preparations are consistent with all these observations. At P3, nearly the entire ME of both *Cdo*$^{+/-}$ and *Cdo*$^{-/-}$ esophagi displayed β-gal$^+$ cells (Fig. S1 H). There was progressive loss of β-gal activity in *Cdo*$^{+/-}$ esophagi at P14 and in the adult, such that in the latter only the very distal region expressed *Cdo*. In contrast, the proximal-to-distal loss of reporter activity was aberrant in *Cdo*$^{-/-}$ esophagi, with considerable retention of expression in proximal regions at both P14 and the adult (Fig. S1 H).

Esophageal skeletal muscle develops in a TZ whose proximal-to-distal progression is aberrant in *Cdo*$^{-/-}$ mice

Cdo$^{-/-}$ mice display delayed skeletal myogenesis during development (Cole et al., 2004). We hypothesized that the mispatterned ME in these mice might have arisen from a similar delay in skeletal muscle differentiation at the TZ. A detailed analysis of skeletal muscle development in the postnatal esophagus has not been performed, so we used IFA to assess different stages of skeletal myogenesis in longitudinal sections of P0 and P7 esophagi, time points prior and subsequent to when *Cdo*$^{-/-}$ mice display an obvious phenotype, respectively. Sections were stained with antibodies to MyoD and Myf5 (markers of determined myoblasts), myogenin (a marker of differentiating myoblasts), and Pax7, which is expressed by multipotent, somitic muscle progenitor cells. Our findings revealed that esophageal skeletal myogenesis is similar to somitic myogenesis.

At both P0 and P7, the distal-most MyoD$^+$ cell was embedded in smooth muscle, and we defined its location as the leading edge of the TZ (Fig. 2, A–C). Most MyoD$^+$ cells were found mixed with dispersed SMCs in the TZ, and their numbers diminished at more proximal locations with the emergence of differentiated skeletal myofibers. We quantified the number of MyoD$^+$ cells within the entire TZ of *Cdo*$^{+/+}$ and *Cdo*$^{-/-}$ esophagi, and they were similar at both P0 and P7 (Fig. 2 D). We also measured the distance from the leading edge of the TZ (the location of the distal-most MyoD$^+$ cell) to the LES. This distance was similar between control and *Cdo*$^{-/-}$ mice at P0, but was significantly longer in mutant mice at P7 (Fig. 2 E). Myogenin$^+$ cells were found in a similar pattern as MyoD$^+$ cells in both *Cdo*$^{+/-}$ and *Cdo*$^{-/-}$ esophagi at P0 and P7 (Fig. 2, F and G; Fig. S2 A). Again, the numbers of such cells at these stages were not different, but the distance from the distal-most myogenin$^+$ cell to the LES was significantly longer in *Cdo*$^{-/-}$ mice than control mice at P7, but not P0. Pax7$^+$ cells were also present in the P7 TZ (Fig. 2, H and I; Fig. S2 B). As seen with the lineage-restricted MyoD$^+$ and myogenin$^+$ cells, the number of Pax7$^+$ cells

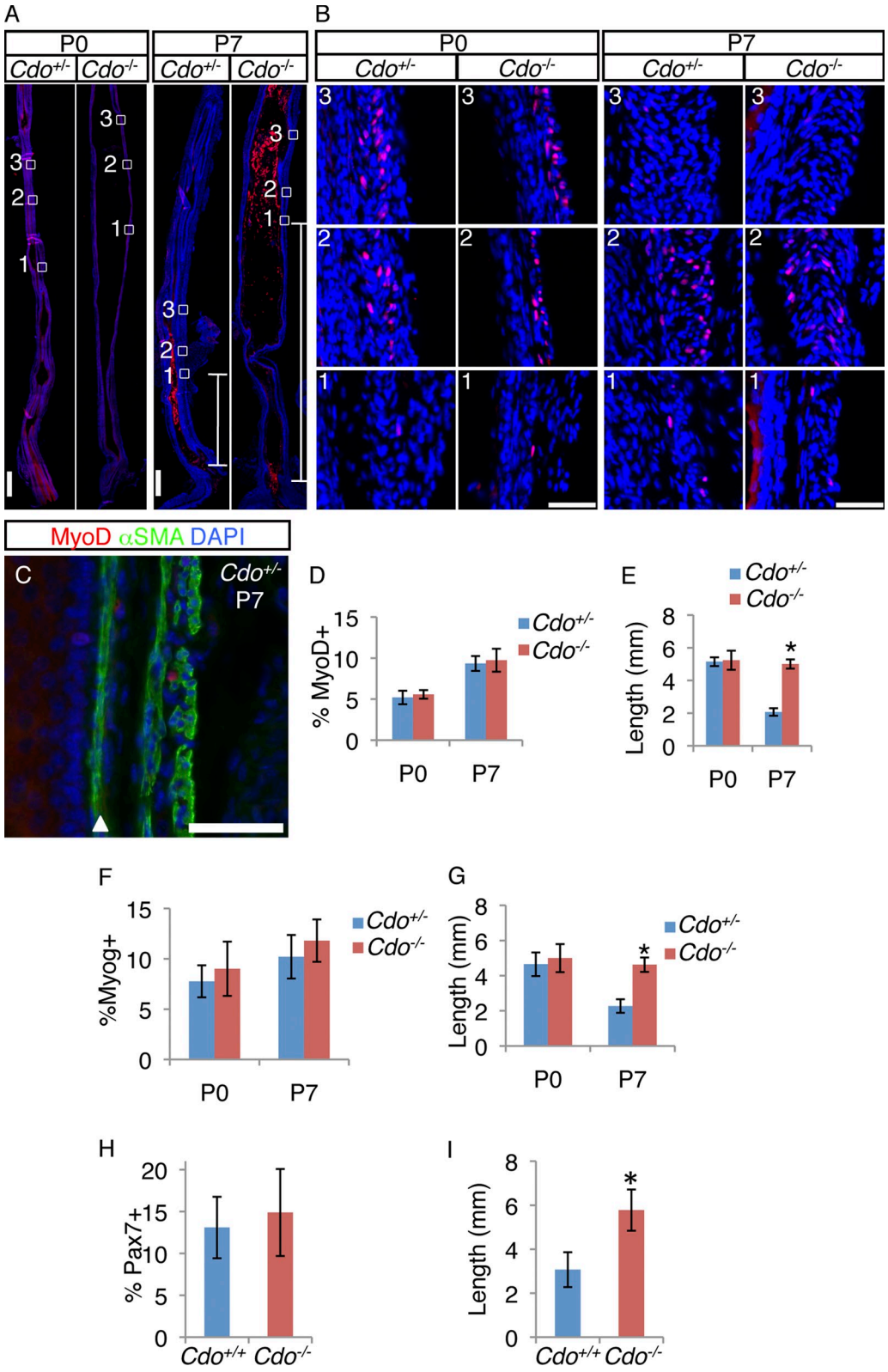

Figure 2. ***Cdo*$^{-/-}$ esophagi have normal numbers of MyoD$^+$, myogenin$^+$, and Pax7$^+$ cells in an aberrantly proximal location.** (A) Longitudinal sections of P0 and P7 *Cdo*$^{+/-}$ and *Cdo*$^{-/-}$ esophagi were stained with antibodies to MyoD (red). Boxed areas correspond to the distal-most MyoD$^+$ cell (1), the region of the transition zone (TZ) with the greatest number of MyoD$^+$ cells (2), and a more proximal region where, by P7, MyoD$^+$ cell numbers diminish (3). These regions are identified by the presence and numbers of MyoD$^+$ cells and are in different locations along the proximal–distal axis in *Cdo*$^{+/-}$ and *Cdo*$^{-/-}$ esophagi. White lines in the P7 micrographs indicate the distance between the distal-most MyoD$^+$ cell and the LES. (B) Higher magnification of boxes 1–3, as indicated. (C) Longitudinal section of P7 *Cdo*$^{+/-}$ esophagus stained with antibodies to MyoD, α-SMA, and with DAPI. The arrowhead denotes the muscularis mucosa. (D, F, and H) Quantification of MyoD$^+$ (D), myogenin$^+$ (F), and Pax7$^+$ (H) cells within the TZ, measured as a percentage of total DAPI$^+$ cells in the ME. (E, G, and I) Quantification of the distance of between the distal-most MyoD$^+$ (E), myogenin$^+$ (G), and Pax7$^+$ (I) cell and the LES. Values in D–I are means ± SD, n = 3–4. *, $P < 0.05$. Bars: (A) 0.5 mm; (B and C) 50 µm.

was similar between $Cdo^{+/-}$ and $Cdo^{-/-}$ esophagi but the distance between the distal-most $Pax7^+$ cell and the LES was significantly greater in $Cdo^{-/-}$ mice than in control mice.

We next investigated cell proliferation in the developing ME. BrdU incorporation was measured after a 2-h pulse at P7. Sections were co-stained with antibodies to Myf5 or α-SMA. $Myf5^+$ cells were restricted to the TZ and, as seen with other markers of the skeletal muscle lineage, $Cdo^{+/-}$ and $Cdo^{-/-}$ mice contained similar numbers of these cells (Fig. 3, A and B). Approximately 30% of $Myf5^+$ cells incorporated BrdU, whereas only ∼3.5% of $\alpha\text{-SMA}^+$ cells did so, in both control and $Cdo^{-/-}$ mice (Fig. 3, A and C). Therefore, TZ myoblasts are proliferative but SMCs are largely quiescent, and loss of Cdo did not alter these properties. As expected, differentiated skeletal myofibers in the proximal ME did not incorporate BrdU. $Pax7^+$ cells in the TZ were also proliferative, as ∼30% were positive for Ki67 (Fig. 3, D and E). Furthermore, ∼26% of $Pax7^+$ cells coexpressed MyoD, but no $Pax7^+$ cells expressed α-SMA, and none were found in the smooth muscle of the distal esophagus (Fig. 3, D and E). Unlike $MyoD^+$ and $myogenin^+$ cells, which were rare in the differentiated skeletal myofibers of the proximal esophagus, scattered $Pax7^+$ cells remained in that region, presumably to establish the population of satellite cells seen in the adult esophagus (Fig. S2 B; Fig. S1 L).

Last, we quantified the number of skeletal myofibers in cross sections through adult esophagi. Although $Cdo^{-/-}$ esophagi were distended, the total number of myofibers was not different from the number seen in $Cdo^{+/-}$ esophagi (Fig. S2, C and D). Taken together, these data are consistent with the conservative notion that esophageal skeletal myogenesis is similar to somitic myogenesis: proliferative $Pax7^+$ cells give rise to lineage-committed $Myf5^+$ and $MyoD^+$ cells, which express myogenin early in the differentiation process to produce SA^+ myofibers. Skeletal muscle progenitors mixed within smooth muscle in the proximal half of the P0 esophagus develop into skeletal myofibers in a TZ that migrates in a proximal-to-distal direction during postnatal maturation of the esophagus. Contrary to our initial hypothesis, skeletal myogenesis per se is not altered in $Cdo^{-/-}$ esophagi, as assessed by numbers of $Pax7^+$, $Myf5^+$, $MyoD^+$, and $myogenin^+$ cells and number of myofibers. Rather, the proximal-to-distal progression of the TZ is laggardly in these mice and ends at an aberrantly proximal position.

Cdo is required for esophageal smooth muscle fascicles to alter their shape and orientation during ME patterning

In the adult wild-type esophagus, most smooth muscle is found in a short, broad segment at the EGJ, where SMCs were bundled into long, thin fascicles that were stacked side by side with an orientation perpendicular to the lumen (Fig. 4, A, C, and E). The smooth muscle–containing portion of adult $Cdo^{-/-}$ esophagi was much longer than in controls (Fig. 1 C; Fig. 4 G) and was thinner, both in the ectopic extension in the esophageal body and at the LES (Fig. 1 I; Fig. 4, B, D, F, and H). Despite the $Cdo^{-/-}$ LES being thinner overall than controls, the smooth muscle fascicles of the mutant LES were arranged side by side and oriented perpendicularly to the lumen, similar to those in the control LES (Fig. 4, E and F). Similar to the LES, the fascicles near the skeletal–smooth muscle boundary in $Cdo^{+/+}$ mice were also arranged side by side and oriented perpendicular to the lumen; in contrast, the fascicles found in the ectopic extension of smooth muscle in $Cdo^{-/-}$ esophagi were arranged end to end with an orientation parallel to the lumen (Fig. 4, C and D). Furthermore, the SMCs within the ectopic smooth muscle region had nearly twice the cross-sectional area of SMCs just distal to the skeletal–smooth muscle boundary in $Cdo^{+/+}$ esophagi or in fascicles at the LES in both $Cdo^{+/+}$ and $Cdo^{-/-}$ mice (Fig. 4 I). Therefore, the aberrantly located SMCs in $Cdo^{-/-}$ esophagi were abnormally large and grouped within fascicles that displayed an inappropriate pattern.

The developmental mechanism whereby esophageal smooth muscle is replaced by skeletal muscle is poorly understood. Given that an intrinsic defect in esophageal skeletal myogenesis was not observed in $Cdo^{-/-}$ mice, and that the esophageal smooth muscle was not merely ectopic but mispatterned, we further explored this phenotypic transition. Loss of esophageal SMCs by apoptosis has been proposed (Wörl and Neuhuber, 2005), but others have failed to observe apoptotic cells during this process (Patapoutian et al., 1995; Kablar et al., 2000; Rishniw et al., 2007). We analyzed longitudinal sections of P7 $Cdo^{+/+}$ and $Cdo^{-/-}$ esophagi by TUNEL assay and by IFA with an antibody to cleaved caspase-3, with thymuses from the same animals as positive controls. Although thymuses from mice of both genotypes displayed easily detectable $TUNEL^+$ and cleaved $caspase\text{-}3^+$ cells, esophagi did not (Fig. S3). Furthermore, the total number of SMCs in $Cdo^{+/+}$ and $Cdo^{-/-}$ esophagi was similar (Fig. 4 J), indicating that the ectopic smooth muscle in the latter mice did not arise as a consequence of failure to remove cells by apoptosis. Moreover, there was little difference in the expression levels of two skeletal muscle–specific genes (*Myh2a* and *Acta1*) and two smooth muscle–specific genes (*Myh11* and *Tagln*) between wild-type and mutant mice as assessed by qRT-PCR analysis of whole adult esophagi (Fig. 4 K). Therefore, despite the mispatterning of the ME, several criteria indicate that there is little difference in the total amount of skeletal and smooth muscle between $Cdo^{+/+}$ and $Cdo^{-/-}$ mice.

The aberrant orientation of the fascicles in the ectopic region of smooth muscle in $Cdo^{-/-}$ esophagi suggested that a process of progressive fascicle reshaping and reorientation may occur during postnatal maturation, accounting for the "disappearance" of smooth muscle. Furthermore, defects in this process might underlie the phenotype of $Cdo^{-/-}$ mice. To assess this possibility, longitudinal sections of P0, P7, and P14 $Cdo^{+/+}$ and $Cdo^{-/-}$ esophagi were stained with an antibody to α-SMA and the shape and orientation of smooth muscle fascicles determined.

At P0, the distal esophagi of $Cdo^{+/+}$ and $Cdo^{-/-}$ mice were similar, with long, thin fascicles arranged end to end and parallel to the lumen, from the TZ to the LES (Fig. 5 A). During postnatal maturation of control esophagi, the TZ descended distally, and smooth muscle fascicles changed their morphology and orientation to the lumen in a distal-to-proximal manner (Fig. 5, A and B). At P7, an intermediate stage of this process was evident just proximal to the LES, where fascicles with a more globular shape were found, followed distally by

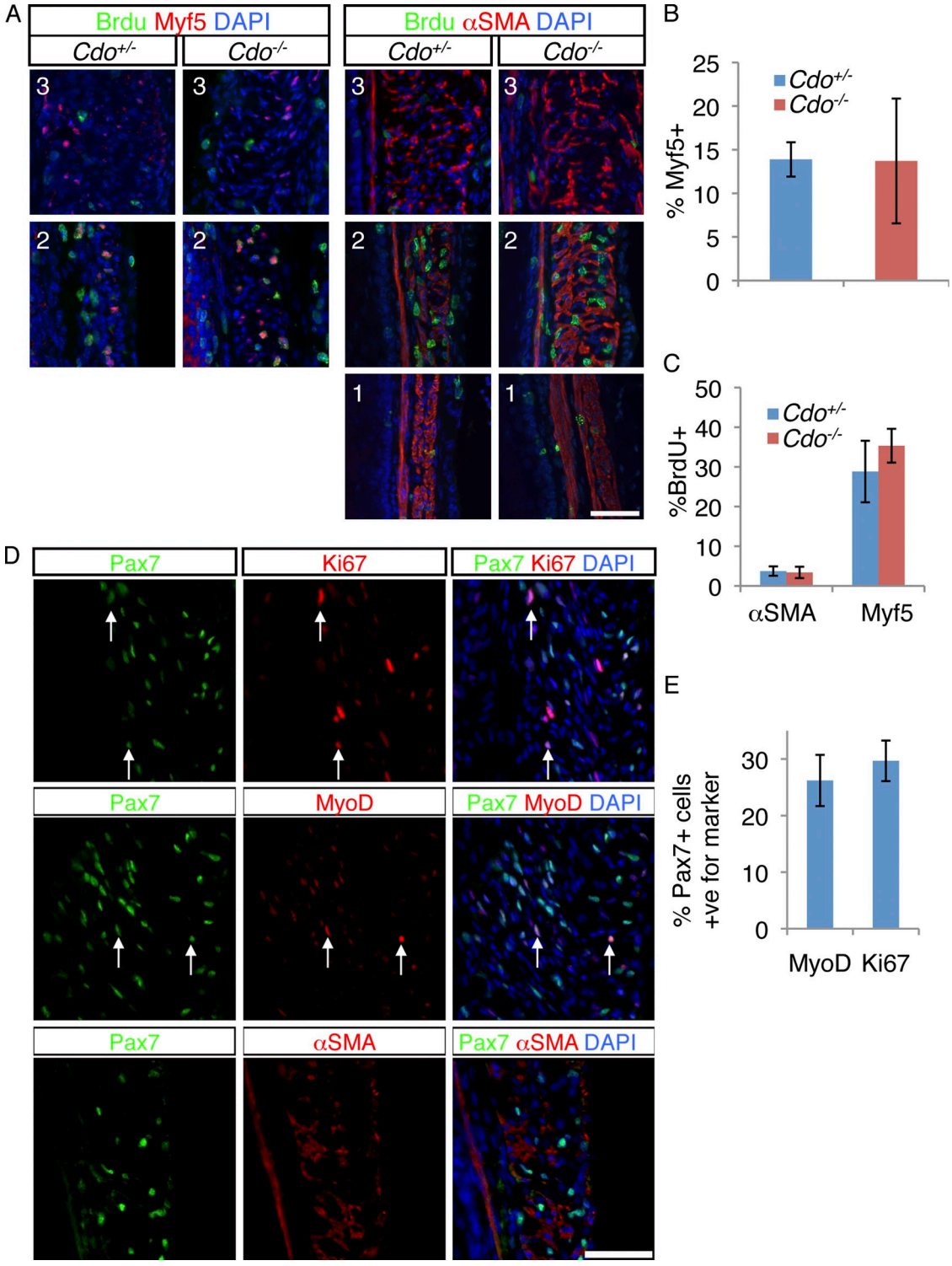

Figure 3. **Proliferative skeletal muscle precursor cells are present in the TZ.** (A) P7 mice were injected with BrdU and 2 h later longitudinal sections of *Cdo*$^{+/-}$ and *Cdo*$^{-/-}$ esophagi were obtained and stained with antibodies to BrdU and Myf5 or α-SMA. The numbers of each panel (1, 2, 3) correspond to the equivalently numbered boxes/panels in Fig. 2. (B) Quantification of Myf5^{+} cells within the TZ, measured as a percentage of total DAPI^{+} cells in the ME. (C) Quantification of percentage of Myf5^{+} and α-SMA^{+} cells that are also positive for BrdU. Values for B and C are means ± SD, $n = 4$. (D) Longitudinal sections of P7 *Cdo*$^{+/+}$ esophagi were stained with antibodies to Pax7 and either Ki67, MyoD, or α-SMA, and with DAPI. Many Pax7^{+} cells coexpressed the proliferation marker Ki67, or the muscle determination marker MyoD (arrows in the respective panels), but Pax7^{+} cells did not express α-SMA. (E) Quantification of the percentage of Pax7^{+} cells in the TZ that are also either Ki67^{+} or MyoD^{+}. Values are means ± SD, $n = 4$.

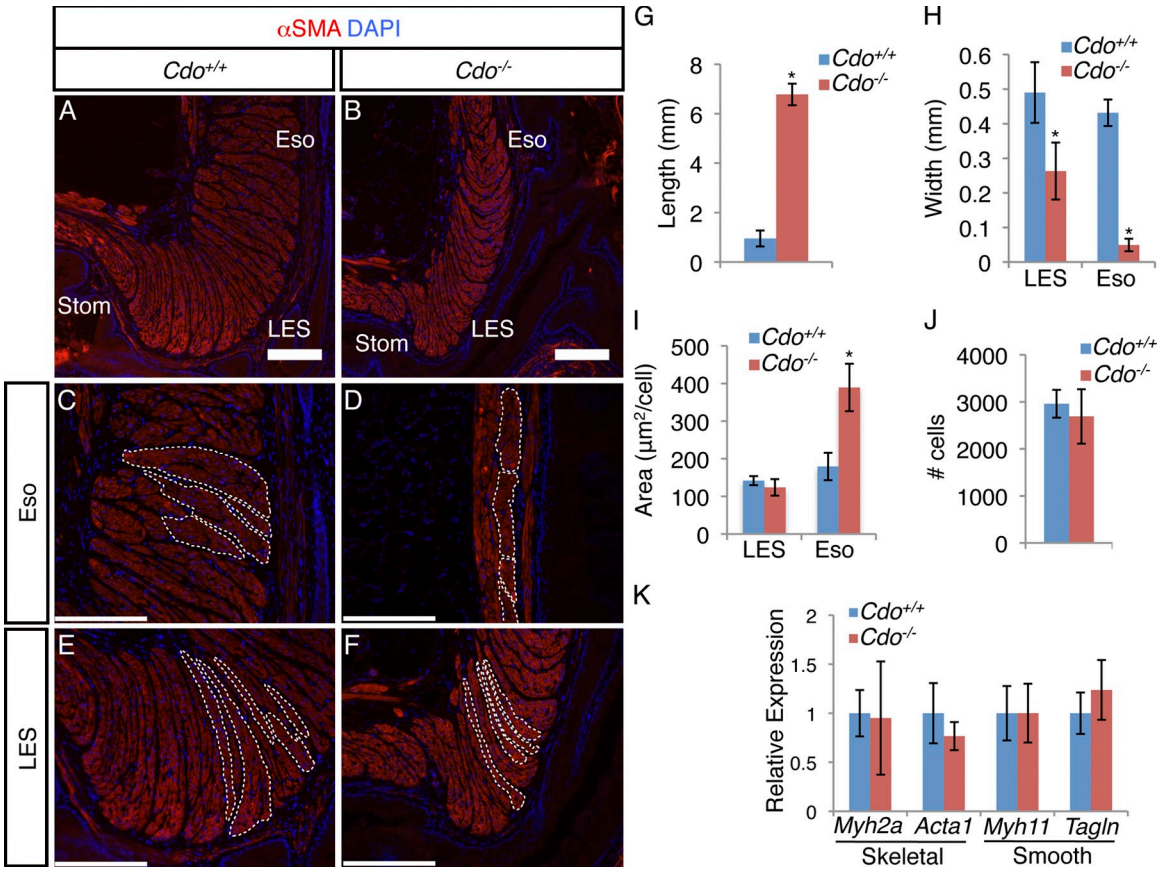

Figure 4. **Adult *Cdo*$^{-/-}$ esophagi have mispatterned smooth muscle.** (A–F) Longitudinal sections of adult *Cdo*$^{+/+}$ and *Cdo*$^{-/-}$ esophagi stained with antibodies to α-SMA and with DAPI. (A and B) SMCs at the LES and esophageal ME just proximal to the LES (Eso) are fasciculated in both *Cdo*$^{+/-}$ and *Cdo*$^{-/-}$ mice, but the smooth muscle layer in *Cdo*$^{-/-}$ esophagi is thinner than controls. Bars, 200 µm. (C–F) Arrangement and orientation of smooth muscle fascicles in the Eso (C and D) and LES (E and F). Individual fascicles are outlined by the white dotted lines. (C and D) In the *Cdo*$^{+/+}$ Eso, fascicles are stacked face to face and are perpendicular to the lumen, whereas in the ectopic smooth muscle extension in *Cdo*$^{-/-}$ esophagi they are end-to-end and parallel to the lumen. (E and F) In the LES, fascicles are face to face and perpendicular to the lumen in both *Cdo*$^{+/+}$ and *Cdo*$^{-/-}$ mice. Bars, 40 µm. (G) Quantification of the distance of between the distal-most SA^{+} cell and the LES in adult esophagi. (H) Quantification of the width of the ME in *Cdo*$^{+/+}$ and *Cdo*$^{-/-}$ esophagi at the LES and in the esophageal body just distal to the skeletal–smooth boundary (Eso). (I) Quantification of the cross-sectional area of individual SMCs in the *Cdo*$^{+/+}$ and *Cdo*$^{-/-}$ LES and Eso. (J) Quantification of the total number of SMCs from the skeletal–smooth muscle boundary to the EGJ from *Cdo*$^{+/+}$ and *Cdo*$^{-/-}$ mice. (K) qRT-PCR analysis of skeletal muscle–specific (*Myh2a* and *Acta1*) and smooth muscle–specific (*Myh11* and *Tagln*) genes from total *Cdo*$^{+/+}$ and *Cdo*$^{-/-}$ esophagus lysates, normalized to expression of 36B4. Values in G–K are means ± SD, $n = 5–6$. *, $P < 0.005$.

fascicles arranged side by side and perpendicular to the lumen. The most proximal fascicles were still in the end-to-end, parallel-to-the-lumen orientation (Fig. 5, A and B). By P14, the smooth muscle fascicles had achieved a pattern similar to that seen in the adult (Fig. 5, A and B). However, the overall area occupied by smooth muscle in *Cdo*$^{+/+}$ esophagi was not different between P7 and P14, consistent with the notion that smooth muscle is not lost during ME patterning (Fig. 5 C). In *Cdo*$^{-/-}$ esophagi fascicular rearrangement failed to occur, with fascicles proximal to the LES remaining in the end-to-end configuration and with an orientation parallel to the lumen (Fig. 5, A and B). Furthermore, *Cdo*$^{-/-}$ SMCs just distal to the TZ had a larger cross-sectional area than control cells at all three time points (Fig. 5 D), suggesting that *Cdo*$^{-/-}$ cells may have a defective shape that in turn contributes to the inability of the fascicles to undergo proper morphogenesis. It is noteworthy that this alteration in cell area was visible at P0, a stage before detectable differences in the location of the TZ or overall esophageal morphology. Consistent with the larger size of *Cdo*$^{-/-}$ SMCs, the overall area occupied by smooth muscle at P7 and P14 in *Cdo*$^{-/-}$ esophagi was larger than that seen in *Cdo*$^{+/+}$ esophagi (Fig. 5 C).

Hh signaling defects are unlikely to be responsible for the esophageal mispatterning in *Cdo*$^{-/-}$ mice

Hh signaling plays important roles in embryonic patterning of the foregut and homeostasis of intestinal smooth muscle (Litingtung et al., 1998; Ramalho-Santos et al., 2000; Zacharias et al., 2011), and Cdo regulates the Hh pathway (Zhang et al., 2006). We therefore analyzed expression of two general, direct target genes of the Hh pathway, *Gli1* and *Ptch1*, during ME patterning at P7. *Gli1* expression was monitored with a *lacZ* knock-in allele, *Ptch1* expression by in situ hybridization. Consistent with previous reports (Ramalho-Santos et al., 2000; Kolterud et al., 2009), high levels of *Gli1* and *Ptch1* were found in the submucosa of the pylorus, and their expression diminished strongly in the associated ME (Fig. S4). *Gli1* and *Ptch1*

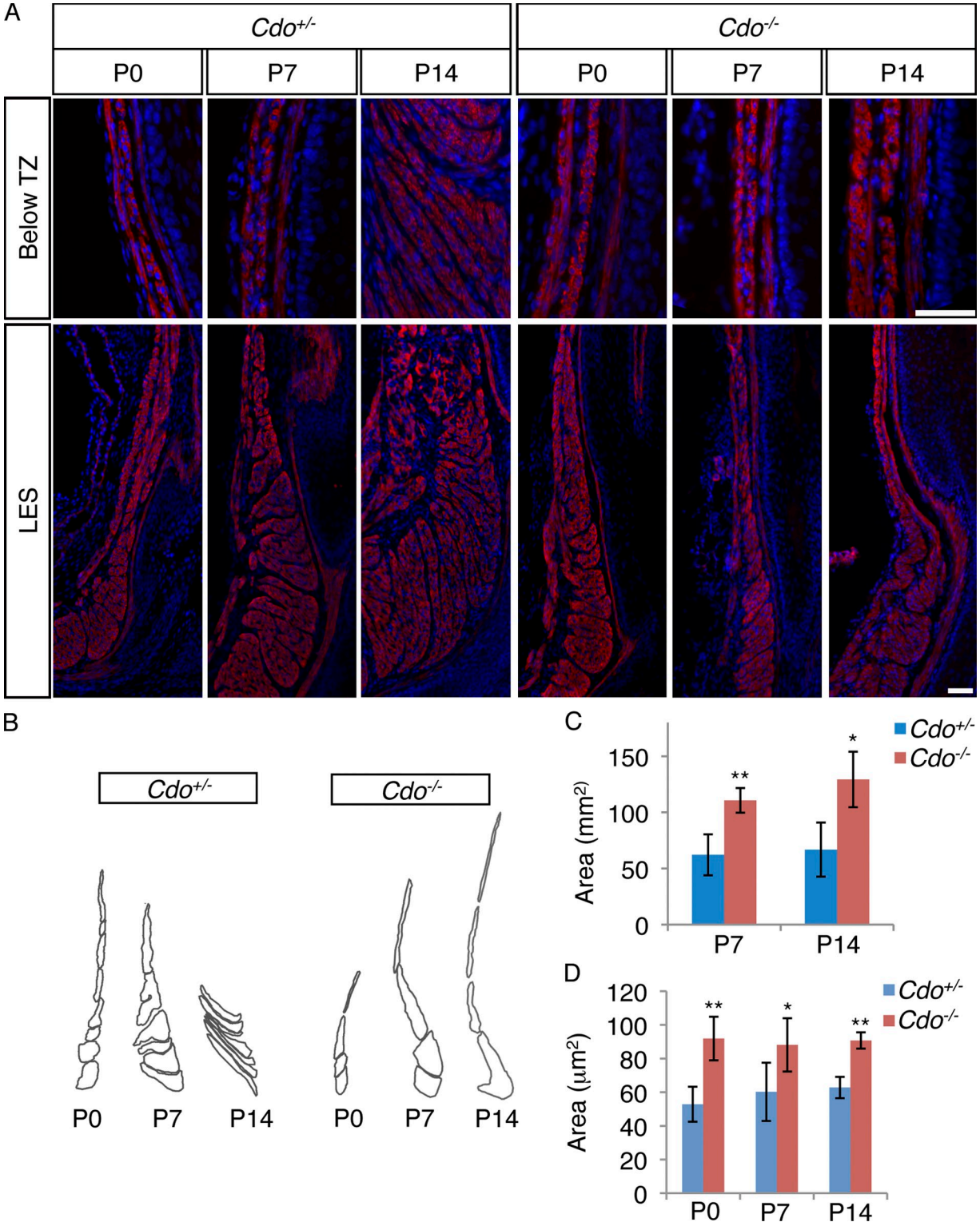

Figure 5. ***Cdo* is required for esophageal smooth muscle fascicle morphogenesis during pattering of the ME.** (A) Longitudinal sections of P0, P7, and P14 $Cdo^{+/-}$ and $Cdo^{-/-}$ esophagi stained with antibodies to α-SMA and with DAPI. Micrographs of the LES and esophageal region just distal to the transition zone (Below TZ) are shown. Between P0 and P14, $Cdo^{+/-}$ smooth muscle fascicles changed their shape and orientation in a distal-to-proximal manner; this process was impaired in $Cdo^{-/-}$ esophagi. Bar, 50 μm. (B) Tracings of smooth muscle fascicles just proximal to the LES in P0, P7, and P14 $Cdo^{+/-}$ and $Cdo^{-/-}$ esophagi indicates the changes in shape and orientation. (C) Quantification of the total cross-sectional smooth muscle area in P7 and P14 $Cdo^{+/-}$ and $Cdo^{-/-}$ esophagi. (D) Quantification of the cross-sectional area of individual SMCs immediately distal to the TZ in $Cdo^{+/-}$ and $Cdo^{-/-}$ mice. Values are means ± SD, n = 3–5. *, $P < 0.05$; **, $P < 0.001$.

expression were also observed in the esophageal submucosa, but at significantly lower levels than in the pylorus (Fig. S4). Furthermore, expression of *Gli1* and *Ptch1* was barely detectable in the esophageal ME, with only occasional positive cells found at the TZ, the smooth muscle distal to the TZ, and the LES (Fig. S4). *Gli1* and *Ptch1* expression in the P7 $Cdo^{-/-}$ pylorus and esophagus were very similar to that of controls (Fig. S4). Taken together, the lack of significant *Gli1* and *Ptch1* expression at the sites of smooth muscle fascicle morphogenesis and lack of alteration in their expression in *Cdo* mutants argues that defects in Hh signaling are unlikely to underlie the phenotype of $Cdo^{-/-}$ mice.

The $Cdo^{-/-}$ LES has a normal density of myenteric neurons but is defective in NO-mediated relaxation

Upon swallowing, nitrergic ($nNOS^+$) myenteric neurons induce relaxation of tonic smooth muscle in the LES to allow passage of food from the esophagus to the stomach (Goyal and Chaudhury, 2008). Achalasia, a chronic condition in which LES relaxation is impaired, is often caused by loss of nitrergic neurons (Park and Vaezi, 2005). As the esophagi of $Cdo^{-/-}$ mice are generally full of ingesta and the LES appears constricted (Fig. 1 A), these animals had an achalasia-like phenotype. We therefore quantified the number of neurons in the LES from adult $Cdo^{+/+}$ and $Cdo^{-/-}$ mice and assessed the ability of ex vivo LES preparations to relax in response to NO.

IFA of LES sections with antibodies to neuron-specific β-tubulin III (TuJ1) and to nNOS revealed that the number and pattern of total and nitrergic neurons, respectively, were similar between control and mutant mice (Fig. S5). Next we performed functional analyses on isolated strips of the LES from $Cdo^{+/+}$ and $Cdo^{-/-}$ mice. LES strips from $Cdo^{+/+}$ mice subjected to electrical field stimulation (EFS) of increasing frequency displayed typical, transient, frequency-dependent relaxation (Fig. 6, B and D). As expected, blocking neuronal production of NO with the NOS inhibitor L-NA completely inhibited EFS-induced relaxation (Fig. 6 C). Although the LES strips from $Cdo^{-/-}$ mice had normal basal tone (Fig. 6 A), they failed to relax in response to EFS (Fig. 6, B and D). Because *Cdo* was expressed in LES SMCs, but not nitrergic neurons, we asked whether the $Cdo^{-/-}$ LES was intrinsically less sensitive to NO. $Cdo^{+/+}$ and $Cdo^{-/-}$ LES smooth muscle strips were treated with increasing doses of the NO-generating compound, sodium nitroprusside (SNP) and relaxation quantified. The dose–response curve for $Cdo^{-/-}$ LES strips was significantly right-shifted as compared with controls (Fig. 6 E). At a concentration of SNP (0.5 µM) that produced a degree of relaxation in $Cdo^{+/+}$ LES strips similar to that achieved maximally by EFS (25–30%), $Cdo^{-/-}$ LES strips were unresponsive (Fig. 6 E). At higher concentrations the $Cdo^{-/-}$ LES strips began to respond, such that at 50 µM they responded similarly to controls (Fig. 6 E). The $Cdo^{-/-}$ LES strips were not resistant to all stimuli, as they responded similarly to controls by contracting dose-dependently when treated with the acetylcholine analogue bethanechol (Fig. 6 F). Collectively, these results indicate that the LES from $Cdo^{-/-}$ mice maintains normal high basal tone but fails to relax in response to endogenous concentrations of NO (Chakder and Rattan, 1993), whether the NO is produced in situ by myenteric neurons or supplied directly in chemical form. The results are consistent with the conclusion that $Cdo^{-/-}$ mice have achalasia as a consequence of defects in SMCs.

Discussion

We report here that mice lacking the cell surface receptor Cdo have a defect in the postnatal developmental process whereby esophageal smooth muscle is replaced by skeletal muscle. Analysis of this process in control and $Cdo^{-/-}$ mice revealed morphogenetic mechanisms that underlie formation of the mature pattern of the esophageal ME. Furthermore, $Cdo^{-/-}$ mice display achalasia, and the LES from such mice is resistant to NO-induced relaxation, suggesting a developmental linkage between ME pattern formation and LES function.

Postnatal development of the esophageal ME

During development of the mammalian esophageal ME, smooth muscle is replaced by skeletal muscle in a proximal-to-distal manner such that, in the mouse, except for a short, broad segment at the EGJ that includes the LES, nearly the entire length of the esophagus is ensheathed in skeletal muscle (Samarasinghe, 1972). The majority of this process occurs between P0 and P14. We have analyzed both skeletal myogenesis and smooth muscle patterning during postnatal ME development in control and $Cdo^{-/-}$ mice to illuminate these processes.

$Myf5^+$ and $MyoD^+$ cells (skeletal myoblasts) are detectable in the most proximal region of the ME as early as E13 (Zhao and Dhoot, 2000b), but it was unclear how proximal-to-distal skeletal myofiber formation occurs. We identified a TZ that contains proliferative skeletal muscle precursor cells and differentiating skeletal myoblasts. These various cells of the skeletal muscle lineage are intermixed with α-SMA^+ SMCs at the distal portion of the TZ, but none of them coexpresses α-SMA. The TZ resides in a more distal position along the esophageal length at P7 than P0. Furthermore, at both time points, differentiated skeletal myofibers are present proximal to the transition zone, whereas SMCs are present distal to it. These observations are consistent with the notion that between E13 and P14, resident skeletal muscle progenitors commit to the myogenic lineage and begin differentiating within a TZ that migrates along the length of the esophagus in a proximal-to-distal manner, leaving differentiated myofibers in its wake (Fig. 7 A). Furthermore, the presence in the TZ of proliferative $Pax7^+$ and $Myf5^+$ cells, plus $MyoD^+$ and $myogenin^+$ cells, none of which expresses α-SMA, is consistent with the conclusions that: (1) in terms of lineage progression, esophageal skeletal muscle development resembles somitic and satellite cell–derived myogenesis; and (2) transdifferentiation does not occur to any appreciable extent, consistent with lineage tracing results (Rishniw et al., 2003).

Despite Cdo's role in promoting skeletal myoblast differentiation during embryogenesis, muscle cell differentiation per se was not altered in $Cdo^{-/-}$ esophagi. Rather, the proximal-to-distal migration of the TZ was impaired in these mice and

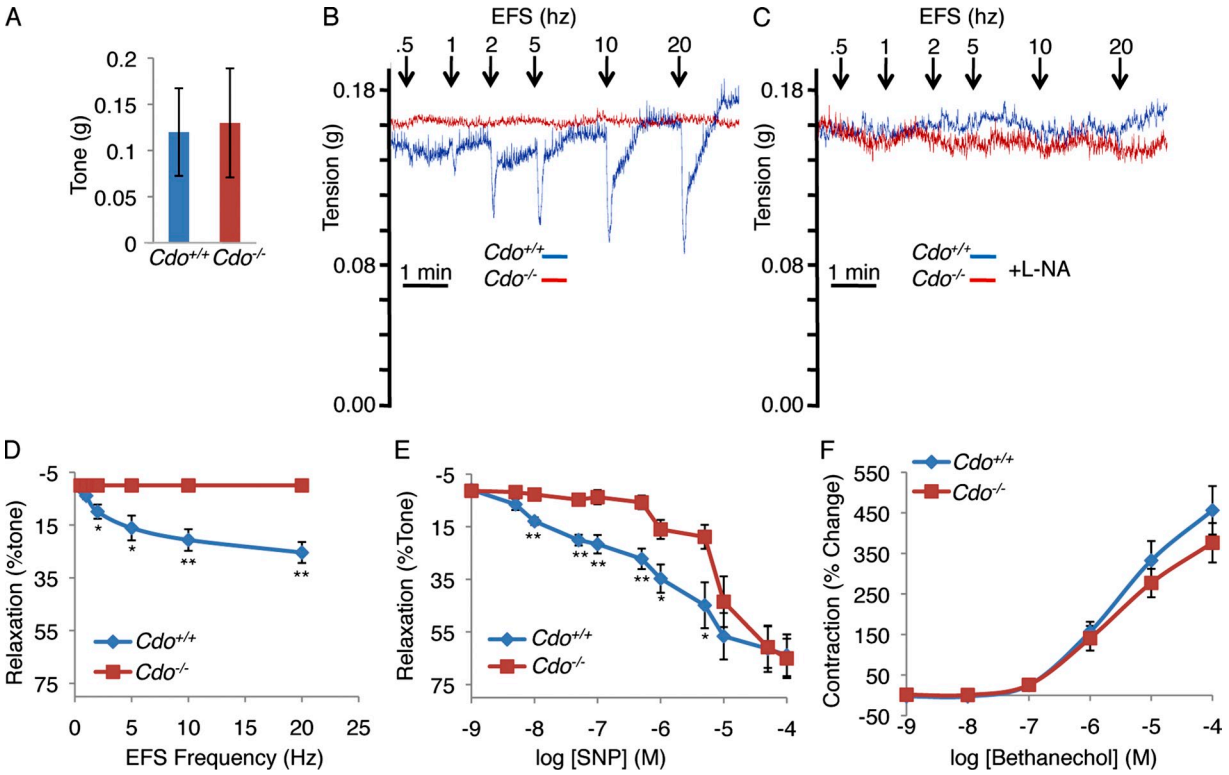

Figure 6. **The *Cdo*$^{-/-}$ LES fails to relax in response to EFS or SNP.** (A) The LES from *Cdo*$^{+/+}$ and *Cdo*$^{-/-}$ mice have similar amplitudes of basal tone. (B) Tension recordings of LES smooth muscle strips. Data shown are from single representative experiments out of five independent experiments on five different LES preparations. Panel D shows results quantified from these experiments. Note that the *Cdo*$^{+/+}$ LES displays transient, frequency-dependent relaxation, which is absent in the *Cdo*$^{-/-}$ LES. (C) Similar to B, except 1 µM L-NA was included. Data shown are from single representative experiments out of five independent experiments on five different LES preparations. (D) Quantification of EFS frequency-dependent relaxation of LES smooth muscle strips from *Cdo*$^{+/+}$ and *Cdo*$^{-/-}$ mice. (E) Quantification of the relaxation response of LES strips from *Cdo*$^{+/+}$ and *Cdo*$^{-/-}$ mice to different concentrations of SNP. (F) Quantification of the contraction response of LES strips from *Cdo*$^{+/+}$ and *Cdo*$^{-/-}$ mice to different concentrations of bethanechol. Values in D–F are means ± SD, $n = 5$. *, $P < 0.05$; **, $P < 0.005$.

ended at an aberrantly proximal position. Analysis of smooth muscle patterning between P0 and P14 offered both an explanation for this phenotype and a mechanism for the fate of esophageal smooth muscle. Proposed mechanisms for the "disappearance" of esophageal smooth muscle are controversial, and include transdifferentiation of SMCs to skeletal muscle cells, removal of SMCs by apoptosis, and a combination of proximal dispersal and distal compaction of SMCs (Patapoutian et al., 1995; Wörl and Neuhuber, 2005; Rishniw et al., 2007). Our findings indicate that between P0 and P14, the distal ME undergoes a morphogenetic process whereby long, thin smooth muscle fascicles arranged end to end and parallel to the lumen rearrange their orientation such that they are ultimately arranged side by side and perpendicular to the lumen. This process of fascicular reorientation results in rearrangement of smooth muscle from a more proximally located and elongated length of ME to a distally located, short, broad segment near and at the EGJ (Fig. 7 B).

Cdo$^{-/-}$ mice are specifically defective in fascicular reorientation, leaving a long, thin smooth muscle extension that occupies the distal ∼20% of the ME. This region does not contain skeletal muscle cells and has an appearance that is reminiscent of an earlier stage of ME development in wild-type animals. Several additional lines of evidence are consistent with the notion that fascicular reorientation is the major process that accounts for smooth muscle fate during maturation of the ME: (1) despite mispatterning of the ME in *Cdo*$^{-/-}$ mice, there was no difference in the levels of skeletal muscle– and smooth muscle–specific transcripts, or numbers of SMCs and skeletal myofibers, between adult *Cdo*$^{+/+}$ and *Cdo*$^{-/-}$ esophagi; (2) as with previous reports (Patapoutian et al., 1995; Kablar et al., 2000; Rishniw et al., 2007), we did not observe any apoptotic cells in the ME; and (3) as discussed in the previous paragraph, we found no evidence for transdifferentiation. These observations indicate that smooth muscle is not lost during postnatal development of the ME. Our results are most similar to those of Rishniw et al. (2007), who proposed that SMCs undergo a combination of proximal dispersal and distal compaction through unknown mechanisms. However, we did not observe significant dispersal of SMCs. Although there is some intermingling of the two cell types at the skeletal–smooth muscle boundary, α-SMA$^+$ cells were not found within the skeletal muscle proximal to this point in adult esophagi. Furthermore, SMCs are not actually compacted, in that the overall area they occupy is similar at P7 and P14; rather, it is their fascicular pattern that is altered.

The process of fascicular reorientation occurred in a distal-to-proximal manner (Fig. 7 B). The signals that trigger this rearrangement of SMCs relative to one another are not known, but we hypothesize that Cdo transduces them. Cdo is well known as a regulator of Hh signaling, but there was little expression of two direct Hh pathway target genes in ME smooth muscle during this

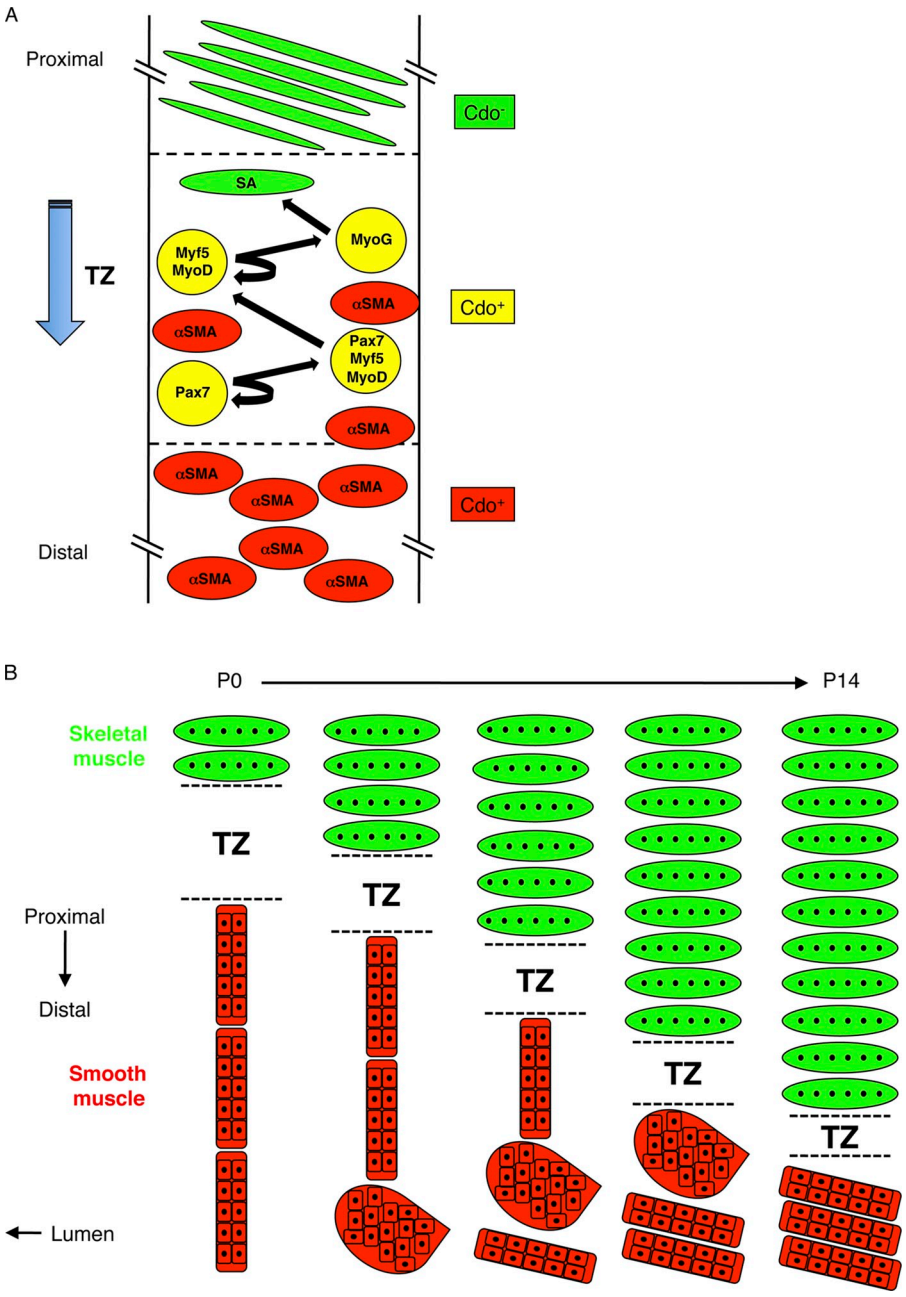

Figure 7. **Models of maturation of the esophageal ME.** (A) Model of skeletal myogenesis in the TZ. The TZ contains proliferating skeletal muscle progenitor (Pax7$^+$) cells, muscle progenitor cells in the process of commitment to the skeletal muscle lineage (Pax7$^+$/Myf5$^+$/MyoD$^+$ cells), skeletal myoblasts (Myf5$^+$/MyoD$^+$ cells), and differentiating skeletal myoblasts (Myog$^+$ cells). The TZ moves in a proximal-to-distal manner, leaving SA$^+$ myofibers in its wake. Smooth muscle (α-SMA$^+$) cells are mainly found distal to the TZ where they undergo fascicular reorientation (see panel B). Some SMCs are also found dispersed within the TZ. Cells of the developing skeletal muscle lineage express Cdo, as do SMCs, but mature skeletal myofibers do not. (B) Model for reorientation of SMC fascicles and proximal-to-distal movement of the TZ between P0 and P14. SMCs of the ME are initially grouped into fascicles that have an end-to-end configuration and an orientation parallel to the lumen. They reorganize in a distal-to-proximal manner via a globular intermediate and culminate in a side-by-side configuration with an orientation that is nearly parallel to the lumen; as a consequence, the fascicles ultimately occupy only the most distal portion of the ME. This process clears a path for the TZ, which migrates distally and produces the multinucleated skeletal myofibers that comprise the great majority of the length of the mature ME.

process in both *Cdo*$^{+/+}$ and *Cdo*$^{-/-}$ mice. Cdo also transduces signals from cadherins to Cdc42 (Kang et al., 2008; Lu and Krauss, 2010). These factors are often involved in regulation of cytoskeletal dynamics of a type that might be required for cell rearrangements. It is of interest in this regard that *Cdo*$^{-/-}$ ME SMCs are apparently larger than control cells and that this is seen at P0, before an overt esophageal phenotype.

Esophageal motility defects in *Cdo*$^{-/-}$ mice

Achalasia is a rare esophageal motility disorder characterized by failure of the LES to relax and consequent impairment of passage of food into the stomach (Park and Vaezi, 2005). It is often accompanied by megaesophagus with distal tapering to a constricted LES. The major cause of achalasia is thought to be loss of ganglionic neurons in the LES, but the etiology is poorly understood. Mice carrying targeted mutations that display achalasia demonstrated that disruption of nitrergic signaling from inhibitory neurons of the myenteric plexus to SMCs of the ME results in achalasia and that the defect can occur both pre- and postjunctionally (Goyal and Chaudhury, 2010). *Cdo*$^{-/-}$ mice display achalasia, but have a normal compliment of nNOS$^+$ neurons in the myenteric plexus. *Cdo*$^{-/-}$ LES smooth muscle strips have normal basal tone but are resistant to NO-induced relaxation, whether the NO is produced in situ from myenteric neurons or supplied directly in chemical form. Therefore, the defect in *Cdo*$^{-/-}$ mice is postjunctional. This phenotype, plus the impairment of smooth muscle fascicular reorientation and lack of effect on skeletal myogenesis, suggests that the esophageal defects in *Cdo*$^{-/-}$ mice are likely to be SMC-autonomous, but conditional mutagenesis will be required to prove this point.

Several mutant lines of mice display achalasia without reported defects in ME patterning (Goyal and Chaudhury, 2010), but the esophagi of mice carrying null mutations in *Col19a1* and *Fzd4* bear a striking resemblance to those of $Cdo^{-/-}$ mice. All three mutants have an aberrantly proximal skeletal–smooth muscle boundary and develop megaesophagus by P8 (Wang et al., 2001; Sumiyoshi et al., 2004). The fact that multiple single-gene mutants have such similar esophageal phenotypes suggests a developmental linkage between ME patterning and LES function. It should be noted, however, that achalasia is not an inevitable consequence of a proximally located skeletal–smooth muscle boundary, as humans normally have a more proximal boundary than mice. Nevertheless, achalasia may have a genetic component (Park and Vaezi, 2005), and it is conceivable that variants in *CDO*, *FZD4*, and *COL19A1* may be predisposing factors. In summary, our findings identify fascicular reorientation as the cell biological mechanism for ME patterning, provide genetic proof that Cdo is required for this process, and link this factor and process to the poorly understood disease, achalasia.

Materials and methods

Mice

Cdo^{tm2Rsk} mice (Cole and Krauss, 2003), which contain an *IRES-lacZ-neo* cassette insertion in the third coding exon, were maintained on a 129S6/SvEvTac background and were genotyped as described previously (Zhang et al., 2006). Homozygous mutants on this background are viable and display mild craniofacial mildline defects (i.e., microform holoprosencephaly) with low penetrance (Zhang et al., 2006). $Gli1^{tm2Alj}$/J (also called $Gli1^{lacZ}$) mice (Bai et al., 2002) were from JAX and were crossed with Cdo^{tm1Rsk} mice, which do not express *lacZ* (Cole and Krauss, 2003). Mice referred to as adult were two to three months of age. All animal work was approved by the Institutional Animal Care and Use Committee (IACUC).

Preparation of frozen sections

Dissected esophagi were prepared for histology either by directly snap-freezing in an isopentane/liquid nitrogen bath or fixing in 2% paraformaldehyde (PFA), washing with PBS, and cryopreserving in 40% sucrose as described previously (Lepper et al., 2009). Frozen tissue blocks were sectioned at 10 or 20 µm and placed on Superfrost Plus slides (Thermo Fisher Scientific).

Immunofluorescence

Frozen sections (10 µm) were immunostained with a protocol adapted from Lepper et al. (2009). Slides were fixed in 2% PFA, washed in PBS, permeabilized in 0.3% Triton/PBS, washed in PBS, blocked in 10% goat serum, and incubated overnight at 4°C with primary antibodies in blocking buffer. Additional M.O.M. blocking (Vector Laboratories) steps were performed according to the manufacturer's instructions when mouse primary antibodies were used. Antibodies used included: rabbit anti–α-SMA (1:200; Abcam), rabbit anti–β-gal (1:50,000; MP Biomedicals), chick anti–β-gal (1:5000; Abcam), rabbit anti-MyoD (1:50; Santa Cruz Biotechnology, Inc.), mouse anti-myogenin (F5D; 1:500; Santa Cruz Biotechnology, Inc.), rabbit anti-Myf5 (1:50; Santa Cruz Biotechnology, Inc.); mouse anti-Pax7 (1:20; Developmental Studies Hybridoma Bank, Iowa City, IA), mouse anti-BrdU (1:200; EMD Millipore), rabbit anti-nNOS (C12H1; 1:500; Cell Signaling Technology), and rabbit anti-Ki67 (1:1,000; Leica). After permeabilization, the following antibodies required an antigen retrieval step of boiling the sections in 10 mM sodium citrate: mouse anti-SA (5C5; 1:1,000; Sigma-Aldrich), mouse anti–α-SMA (clone 1A4; 1:10,000; Sigma-Aldrich), mouse anti–β-tubulin III (TuJ1; 1:500; Sigma-Aldrich), and rabbit cleaved caspase-3 (Asp175; 1:1,000; Cell Signaling Technology). Fluorescent secondary antibodies were from Invitrogen and used at 1:1,000: goat anti–rabbit Alexa Fluor 568, goat anti–mouse Alexa Fluor 488, goat anti–mouse IgG1 Alexa Fluor 488, and goat anti–chicken Alexa Fluor 568. Nuclei were fluorescently labeled with DAPI and mounted with flouroG anti-fade medium (SouthernBiotech). TUNEL assay was performed using the In Situ Cell Death Detection kit from Roche. For BrdU incorporation experiments, mice were injected with 100 µg BrdU per g body weight and sacrificed 2 h later. IFA was performed as above, except that before blocking, sections were incubated in 2 N HCl in PBS for 40 min at 37°C, followed by washing in PBST.

In situ hybridization

Synthesis of digoxigenin-labeled RNA probes and in situ hybridization for *Ptch1* and *Cdo* was performed as described previously (Zhang et al., 2011). Frozen sections (20 µm) were fixed in 4% PFA, treated with 0.1% DEPC, permeabilized with 1 mg/ml proteinase K in PBS, and quenched in 2 mg/ml glycine with washes in PBS between each step. Slides were then post-fixed in 4% PFA, washed, and prehybridized in 50% formamide, 5× SSC, 50 µg/ml yeast tRNA, 50 µg/ml heparin, and 0.25% SDS for 1 h at 58°C. After hybridization (0.5 µg/ml of probe) for 16 h at 58°C, slides were washed in 5×, 2×, and 0.2× SSC at 65°C, allowed to cool to room temperature, washed in TBST, blocked in 1% Roche blocking reagent with 10% lamb serum in TBST for 1 h, and incubated with anti-digoxigenin antibody conjugated with alkaline phosphatase (1:2,000; Roche) for 16 h at 4°C in blocking buffer. Sections were then washed in TBST, and washed and stained in a solution with NBT and BCIP (Roche).

β-Gal staining

Esophagi were either snap-frozen, sectioned, and fixed in 0.5% gluteraldehyde for 5 min on ice, or prepared for whole-mount staining by fixing in 2% PFA for 2 h at 4°C. After fixation samples were washed in PBS and stained in 1 mg/ml X-gal, 5 mM K_3FeCN, 5 mM K_4FeCN, 2 mM $MgCl_2$, 0.02% NP-40, 0.01% sodium deoxycholate ,and PBS at 37°C.

Microscopy

Microscopy was performed at the Mount Sinai Microscopy Shared Resource Facility using Axioplan2 and Axioplan2 IE microscopes (Carl Zeiss) equipped with 10, 20, 40, and 100× objective lenses that had numerical apertures of 0.5, 0.8, 0.75, and 1.4, respectively. Images were acquired at room temperature with a camera (Axio Cam MRm; Carl Zeiss) for fluorescence and a camera for brightfield (Axio Cam MRc; Carl Zeiss). Mosaic images were compiled using the stitching feature in the AxioVision software, with the exception of Fig. 1 K where some misaligned images in blank areas surrounding the tissue section were manually assembled. Total area of fluorescence was determined by thresholding using MetaMorph software. The average smooth muscle cross-sectional cell area in the ME in different regions of the distal esophagus was calculated as the total area of α-SMA$^+$ fluorescence divided by the total number of smooth muscle nuclei. The total number of SMCs at the EGJ and the distal esophageal body were calculated by dividing the total area of α-SMA$^+$ fluorescence by the average SMC area determined for each region. The total number of SMCs in the distal esophagus was calculated as the sum total of SMCs at the EGJ and the distal esophageal body. All other measurements and tracings of smooth muscle fascicles were done using ImageJ software (National Institutes of Health).

qRT-PCR

RNA was extracted from esophageal tissue with Trizol and was reverse transcribed with the SuperScript III First Strand Synthesis System (Invitrogen). qRT-PCR was performed using PerfeCTa SYBR Green FastMix (Quanta Biosciences) with a thermal cycler (iCycler iQ5; Bio-Rad Laboratories). Relative gene expression was calculated using the Plaffl method. Primer sequences for *Myh2a* and *Acta1* were from the Harvard Primer Bank (PrimerBank ID no. 21489941a1 and 133893192b1, respectively; Spandidos et al., 2010). For *Myh11*, the sequences for the forward and reverse primers were 5′-AAGGAAACACCAAGGTCAAGCAGC-3′ and 5′-TCATTGCTCTCTGTGGCCTCATCT-3′, respectively. For *Tagln*, the sequences for the forward and reverse primers were 5′-TCTAATGGCTTTGGGCAGTTTGGC-3′ and 5′-TTTGAAGGCCAATGACGTGCTTCC-3′, respectively. Primers sequences for 36B4 were from Wu et al. (2008).

LES physiology

The changes in isometric tension of isolated smooth muscle strips of LES placed in an organ bath was measured in response to EFS and drugs as described by Sumiyoshi et al. (2004). The esophagus and stomach were removed immediately after sacrifice and placed in oxygenated (95% O_2/5% CO_2) Krebs' physiological solution (KPS). The esophagus and stomach were cut open along the greater curvature and pinned down with the mucosa facing up. Using a dissection microscope, ∼1 × 3-mm strips of LES were prepared from the EGJ and placed in organ baths with one end

anchored to the bottom and the other end tied to a force transducer with thread. These smooth muscle strips were initially stretched to 0.5 g and allowed to equilibrate for 1 h. The basal tone was measured as the loss in tension by replacing KPS buffer with a modified Ca^{+2}-free buffer ($CaCl_2$ was substituted with $MgCl_2$). Responses to EFS (10 V, 0.5-ms pulse duration, 4-s train) were measured under NANC (nonadrenergic, noncholinergic) conditions (in the presence of 1 µM atropine and 1 µM guanethidine). All of the LES smooth muscle strips used maintained tone throughout the experiment. Changes in the basal LES tone were also measured following increasing concentrations of SNP or bethanechol, in a cumulative manner.

Online supplemental material

Fig. S1 is related to Fig. 1 and shows the expression of *Cdo* in the postnatal esophagus. Fig. S2 is related to Fig. 2 and shows that similar numbers of myogenin$^+$ cells, Pax7$^+$ cells and skeletal myofibers are present in P7 *Cdo*$^{+/+}$ and *Cdo*$^{-/-}$ esophagi. Fig. S3 is related to Fig. 4 and shows that apoptotic cells are not found in the developing esophageal ME. Fig. S4 is related to Fig. 5 and shows that canonical Hh signaling is largely absent in the developing esophageal ME of *Cdo*$^{+/+}$ and *Cdo*$^{-/-}$ esophagi. Fig. S5 is related to Fig. 6 and shows that the *Cdo*$^{-/-}$ LES has a normal density of myenteric neurons. Videos 1 and 2 are related to Fig. 1 and show morphology and peristaltic contraction of *Cdo*$^{+/+}$ and *Cdo*$^{-/-}$ esophagi, respectively. Online supplemental material is available at http://www.jcb.org/cgi/content/full/jcb.201301005/DC1.

We thank P. Wassarman and F. Ramirez for critical comments on the manuscript, N. Mor for help with LES dissection, and the Mount Sinai Microscopy Shared Resource Facility for microscopy.

This work was supported by grants from the National Institutes of Health (R01AR46207) and the Muscular Dystrophy Association to R.S. Krauss and the National Institutes of Health (R01DK035385) to S. Rattan.

Submitted: 2 January 2013
Accepted: 11 March 2013

References

Bai, C.B., W. Auerbach, J.S. Lee, D. Stephen, and A.L. Joyner. 2002. Gli2, but not Gli1, is required for initial Shh signaling and ectopic activation of the Shh pathway. *Development*. 129:4753–4761. http://dx.doi.org/10.1242/dev.00115

Chakder, S., and S. Rattan. 1993. Release of nitric oxide by activation of nonadrenergic noncholinergic neurons of internal anal sphincter. *Am. J. Physiol.* 264:G7–G12.

Cole, F., and R.S. Krauss. 2003. Microform holoprosencephaly in mice that lack the Ig superfamily member Cdon. *Curr. Biol.* 13:411–415. http://dx.doi.org/10.1016/S0960-9822(03)00088-5

Cole, F., W. Zhang, A. Geyra, J.-S. Kang, and R.S. Krauss. 2004. Positive regulation of myogenic bHLH factors and skeletal muscle development by the cell surface receptor CDO. *Dev. Cell*. 7:843–854. http://dx.doi.org/10.1016/j.devcel.2004.10.009

Goyal, R.K., and A. Chaudhury. 2008. Physiology of normal esophageal motility. *J. Clin. Gastroenterol.* 42:610–619. http://dx.doi.org/10.1097/MCG.0b013e31816b444d

Goyal, R.K., and A. Chaudhury. 2010. Pathogenesis of achalasia: lessons from mutant mice. *Gastroenterology*. 139:1086–1090. http://dx.doi.org/10.1053/j.gastro.2010.08.013

Kablar, B., S. Tajbakhsh, and M.A. Rudnicki. 2000. Transdifferentiation of esophageal smooth to skeletal muscle is myogenic bHLH factor-dependent. *Development*. 127:1627–1639.

Kang, J.-S., M. Gao, J.L. Feinleib, P.D. Cotter, S.N. Guadagno, and R.S. Krauss. 1997. CDO: an oncogene-, serum-, and anchorage-regulated member of the Ig/fibronectin type III repeat family. *J. Cell Biol.* 138:203–213. http://dx.doi.org/10.1083/jcb.138.1.203

Kang, J.-S., P.J. Mulieri, C. Miller, D.A. Sassoon, and R.S. Krauss. 1998. CDO, a robo-related cell surface protein that mediates myogenic differentiation. *J. Cell Biol.* 143:403–413. http://dx.doi.org/10.1083/jcb.143.2.403

Kang, J.-S., G.-U. Bae, M.-J. Yi, Y.-J. Yang, J.-E. Oh, G. Takaesu, Y.T. Zhou, B.C. Low, and R.S. Krauss. 2008. A Cdo-Bnip-2-Cdc42 signaling pathway regulates p38α/β MAPK activity and myogenic differentiation. *J. Cell Biol.* 182:497–507. http://dx.doi.org/10.1083/jcb.200801119

Katori, Y., B.H. Cho, C.H. Song, M. Fujimiya, G. Murakami, and T. Kawase. 2010. Smooth-to-striated muscle transition in human esophagus: an immunohistochemical study using fetal and adult materials. *Ann. Anat.* 192:33–41. http://dx.doi.org/10.1016/j.aanat.2009.09.007

Kolterud, A., A.S. Grosse, W.J. Zacharias, K.D. Walton, K.E. Kretovich, B.B. Madison, M. Waghray, J.E. Ferris, C. Hu, J.L. Merchant, et al. 2009. Paracrine Hedgehog signaling in stomach and intestine: new roles for hedgehog in gastrointestinal patterning. *Gastroenterology*. 137:618–628. http://dx.doi.org/10.1053/j.gastro.2009.05.002

Krauss, R.S. 2010. Regulation of promyogenic signal transduction by cell-cell contact and adhesion. *Exp. Cell Res.* 316:3042–3049. http://dx.doi.org/10.1016/j.yexcr.2010.05.008

Lagha, M., T. Sato, L. Bajard, P. Daubas, M. Esner, D. Montarras, F. Relaix, and M. Buckingham. 2008. Regulation of skeletal muscle stem cell behavior by Pax3 and Pax7. *Cold Spring Harb. Symp. Quant. Biol.* 73:307–315. http://dx.doi.org/10.1101/sqb.2008.73.006

Lepper, C., S.J. Conway, and C.M. Fan. 2009. Adult satellite cells and embryonic muscle progenitors have distinct genetic requirements. *Nature*. 460:627–631. http://dx.doi.org/10.1038/nature08209

Litingtung, Y., L. Lei, H. Westphal, and C. Chiang. 1998. Sonic hedgehog is essential to foregut development. *Nat. Genet.* 20:58–61. http://dx.doi.org/10.1038/1717

Lu, M., and R.S. Krauss. 2010. N-cadherin ligation, but not Sonic hedgehog binding, initiates Cdo-dependent p38α/β MAPK signaling in skeletal myoblasts. *Proc. Natl. Acad. Sci. USA*. 107:4212–4217. http://dx.doi.org/10.1073/pnas.0908883107

Mulieri, P.J., A. Okada, D.A. Sassoon, S.K. McConnell, and R.S. Krauss. 2000. Developmental expression pattern of the *cdo* gene. *Dev. Dyn.* 219:40–49. http://dx.doi.org/10.1002/1097-0177(2000)9999:9999<::AID-DVDY1032>3.0.CO;2-M

Park, W., and M.F. Vaezi. 2005. Etiology and pathogenesis of achalasia: the current understanding. *Am. J. Gastroenterol.* 100:1404–1414. http://dx.doi.org/10.1111/j.1572-0241.2005.41775.x

Parker, M.H., P. Seale, and M.A. Rudnicki. 2003. Looking back to the embryo: defining transcriptional networks in adult myogenesis. *Nat. Rev. Genet.* 4:497–507. http://dx.doi.org/10.1038/nrg1109

Patapoutian, A., B.J. Wold, and R.A. Wagner. 1995. Evidence for developmentally programmed transdifferentiation in mouse esophageal muscle. *Science*. 270:1818–1821. http://dx.doi.org/10.1126/science.270.5243.1818

Ramalho-Santos, M., D.A. Melton, and A.P. McMahon. 2000. Hedgehog signals regulate multiple aspects of gastrointestinal development. *Development*. 127:2763–2772.

Rishniw, M., H.B. Xin, K.Y. Deng, and M.I. Kotlikoff. 2003. Skeletal myogenesis in the mouse esophagus does not occur through transdifferentiation. *Genesis*. 36:81–82. http://dx.doi.org/10.1002/gene.10198

Rishniw, M., P.W. Fisher, R.M. Doran, E. Meadows, W.H. Klein, and M.I. Kotlikoff. 2007. Smooth muscle persists in the muscularis externa of developing and adult mouse esophagus. *J. Muscle Res. Cell Motil.* 28:153–165. http://dx.doi.org/10.1007/s10974-007-9112-y

Samarasinghe, D.D. 1972. Some observations on the innervation of the striated muscle in the mouse oesophagus—an electron microscopy study. *J. Anat.* 112:173–184.

Spandidos, A., X. Wang, H. Wang, and B. Seed. 2010. PrimerBank: a resource of human and mouse PCR primer pairs for gene expression detection and quantification. *Nucleic Acids Res.* 38(Database issue):D792–D799. http://dx.doi.org/10.1093/nar/gkp1005

Sumiyoshi, H., N. Mor, S.Y. Lee, S. Doty, S. Henderson, S. Tanaka, H. Yoshioka, S. Rattan, and F. Ramirez. 2004. Esophageal muscle physiology and morphogenesis require assembly of a collagen XIX-rich basement membrane zone. *J. Cell Biol.* 166:591–600. http://dx.doi.org/10.1083/jcb.200402054

Takaesu, G., J.S. Kang, G.U. Bae, M.J. Yi, C.M. Lee, E.P. Reddy, and R.S. Krauss. 2006. Activation of p38α/β MAPK in myogenesis via binding of the scaffold protein JLP to the cell surface protein Cdo. *J. Cell Biol.* 175:383–388. http://dx.doi.org/10.1083/jcb.200608031

Tenzen, T., B.L. Allen, F. Cole, J.-S. Kang, R.S. Krauss, and A.P. McMahon. 2006. The cell surface membrane proteins Cdo and Boc are components and targets of the Hedgehog signaling pathway and feedback network in mice. *Dev. Cell*. 10:647–656. http://dx.doi.org/10.1016/j.devcel.2006.04.004

Wang, Y., D. Huso, H. Cahill, D. Ryugo, and J. Nathans. 2001. Progressive cerebellar, auditory, and esophageal dysfunction caused by targeted disruption of the frizzled-4 gene. *J. Neurosci.* 21:4761–4771.

Wörl, J., and W.L. Neuhuber. 2005. Ultrastructural analysis of the smooth-to-striated transition zone in the developing mouse esophagus: emphasis on apoptosis of smooth and origin and differentiation of striated muscle cells. *Dev. Dyn.* 233:964–982. http://dx.doi.org/10.1002/dvdy.20436

Wu, Y., J.Y. Kim, S. Zhou, and C.M. Smas. 2008. Differential screening identifies transcripts with depot-dependent expression in white adipose tissues. *BMC Genomics*. 9:397. http://dx.doi.org/10.1186/1471-2164-9-397

Zacharias, W.J., B.B. Madison, K.E. Kretovich, K.D. Walton, N. Richards, A.M. Udager, X. Li, and D.L. Gumucio. 2011. Hedgehog signaling controls

homeostasis of adult intestinal smooth muscle. *Dev. Biol.* 355:152–162. http://dx.doi.org/10.1016/j.ydbio.2011.04.025

Zhang, W., J.-S. Kang, F. Cole, M.J. Yi, and R.S. Krauss. 2006. Cdo functions at multiple points in the Sonic Hedgehog pathway, and Cdo-deficient mice accurately model human holoprosencephaly. *Dev. Cell*. 10:657–665. http://dx.doi.org/10.1016/j.devcel.2006.04.005

Zhang, W., M. Hong, G.-U. Bae, J.-S. Kang, and R.S. Krauss. 2011. *Boc* modifies the holoprosencephaly spectrum of *Cdo* mutant mice. *Dis Model Mech*. 4:368–380. http://dx.doi.org/10.1242/dmm.005744

Zhao, W., and G.K. Dhoot. 2000a. Both smooth and skeletal muscle precursors are present in foetal mouse oesophagus and they follow different differentiation pathways. *Dev. Dyn.* 218:587–602. http://dx.doi.org/10.1002/1097-0177(2000)9999:9999<::AID-DVDY1019>3.0.CO;2-3

Zhao, W., and G.K. Dhoot. 2000b. Skeletal muscle precursors in mouse esophagus are determined during early fetal development. *Dev. Dyn.* 219:10–20. http://dx.doi.org/10.1002/1097-0177(2000)9999:9999<::AID-DVDY1029>3.0.CO;2-2